

PAPER

High sensitive detection of copper II ions using D-penicillamine-coated gold nanorods based on localized surface plasmon resonance

To cite this article: Yoochan Hong *et al* 2018 *Nanotechnology* **29** 215501

View the [article online](#) for updates and enhancements.

Related content

- [Ultrasensitive, highly selective, and real-time detection of protein using functionalized CNTs as MIP platform for FOSPR-based biosensor](#)
Anisha Pathak, Shama Parveen and Banshi D Gupta
- [Protein Based Localized Surface Plasmon Resonance Gas Sensing](#)
Meisam Omid, Gh. Amoabediny, F. Yazdian et al.
- [Morphological control of gold nanorods via thermally driven bi-surfactant growth and application for detection of heavy metal ions](#)
Hao Huang, Huiyi Li, Huaiyu Wang et al.



IOP | ebooks™

Bringing you innovative digital publishing with leading voices to create your essential collection of books in STEM research.

Start exploring the collection - download the first chapter of every title for free.

High sensitive detection of copper II ions using D-penicillamine-coated gold nanorods based on localized surface plasmon resonance

Yoochan Hong^{1,4}, Seongjae Jo^{2,4}, Joohyung Park², Jinsung Park^{2,5}  and Jaemoon Yang^{3,5} 

¹ Department of Medical Device, Daegu Research Center for Medical Devices and Green Energy, Korea Institute of Machinery & Materials (KIMM), Daegu 42994, Republic of Korea

² Department of Control and Instrumentation Engineering, Korea University, Sejong 30019, Republic of Korea

³ Department of Radiology, College of Medicine, Yonsei University, Seoul 03722, Republic of Korea

E-mail: shinedew@korea.ac.kr and 177hum@yuhs.ac

Received 29 December 2017, revised 16 February 2018

Accepted for publication 7 March 2018

Published 28 March 2018



CrossMark

Abstract

In this paper, we describe the development of a nanoplasmonic biosensor based on the localized surface plasmon resonance (LSPR) effect that enables a sensitive and selective recognition of copper II ions. First, we fabricated the nanoplasmonics as LSPR substrates using gold nanorods (GNR) and the nano-adsorption method. The LSPR sensitivity of the nanoplasmonics was evaluated using various solvents with different refractive indexes. Subsequently, D-penicillamine (DPA)—a chelating agent of copper II ions—was conjugated to the surface of the GNR. The limit of detection (LOD) for the DPA-conjugated nanoplasmonics was 100 pM. Furthermore, selectivity tests were conducted using various divalent cations, and sensitivity tests were conducted on the nanoplasmonics under blood-like environments. Finally, the developed nanoplasmonic biosensor based on GNR shows great potential for the effective recognition of copper II ions, even in human blood conditions.

Supplementary material for this article is available [online](#)

Keywords: localized surface plasmon resonance, copper II ion, D-penicillamine, gold nanorods

(Some figures may appear in colour only in the online journal)

1. Introduction

With the advancement of technology, the use of metals is increasing, along with problems associated with the presence of metals in the human body [1, 2]. In the past, diseases caused by heavy metals such as lead, mercury, and cadmium posed the most significant problem [3]. However, many studies also indicate that, nowadays, non-heavy metals such as aluminum, silver, and copper can also cause damage to the human body [4, 5].

Copper exists in the human body and is composed of several organisms: cytochrome c oxidase, the respiratory enzyme, and ceruloplasmin, which is essential for iron metabolism [6]. For example, the body of a healthy individual maintains a 14.5–18.0 μM concentration range of copper in the blood [7–9]. In addition to iron metabolism regulated by copper, numerous diseases are linked to the deficiency of trace elements. An elevation of the concentration of copper II ions in the human body can lead to Wilson's disease [10], and the concentration of copper in cancer patients was determined to be higher than that of a healthy person (breast cancer: $23.9 \pm 3.4 \mu\text{M}$; pulmonary cancer: $22.9 \pm 6.2 \mu\text{M}$; gastrointestinal cancer: $20.1 \pm 3.2 \mu\text{M}$;

⁴ These authors equally contributed to this work.

⁵ Authors to whom any correspondence should be addressed.

gynecological cancer: $26.2 \pm 7.0 \mu\text{M}$) [7]. A decrease in the concentration of copper can cause Menkes disease and horn syndrome, and an individual with Alzheimer's disease has a lower concentration of copper than a healthy person [8, 11]. Moreover, according to a recent study, copper is essential to oncogenic BRAF signaling and tumorigenesis [12]. In addition, research for the destruction of breast cancer by targeting copper has been reported [13]. Accordingly, studies monitoring the concentration of copper II ions in the blood are important.

There have been many studies on the methodologies for the detection of copper. The inductively coupled plasma mass spectrometer is the most commonly used method [14, 15], but this equipment is very expensive, and the samples must be dissolved in a separate solvent in order to obtain accurate results; therefore, it is not suitable for continuous measurements. The atomic absorption spectrometer requires its own lamp for elemental analysis, and measurements are time-consuming because the lamp must warm up; for these reasons this method is also not suitable [16]. Further, copper can also be detected by colorimetry through gold nanoparticles [17] or bio-conjugated particles [18], electrochemistry using organic molecules [19] or DNAzyme [20], and the fluorescence method using gold nanoclusters [19] or copper nanoparticles [21]. Although many studies have measured copper II ions in blood samples, monitoring is difficult.

In this study, we developed a recognition method with high sensitivity and selectivity from blood-like samples. We measured copper II ions using a plasmon shift by localized surface plasmon resonance (LSPR). LSPR is a special optical property of metal nanoparticles that detects target molecules by observing a shift in the extinction or scattering spectrum [22]. We selected gold nanorods (GNR) owing to their strong absorption in the near infrared spectral region which reduces the influence of visible light [23]. Moreover, in order to selectively detect copper II ions, we used an upgraded system to detect copper in a blood-like sample compared to previously reported works [24, 25]. On the other hand, D-penicillamine (DPA) is a chelator that selectively binds to copper II ions, and it is possible to lower the copper concentration in the human body using DPA; it has been used as a therapeutic agent for Wilson's disease [26]. Therefore, we assumed that the DPA may bind the copper in the blood-like sample. To ensure that the nanoplasmonic substrates (GNR covered with DPA) could measure the copper II ions in the blood sample, samples were prepared by human serum albumin (HSA) (40 g L^{-1}), which accounts for 60% of serum proteins. The DPA-covered nanoplasmonics recognized the copper II ions in deionized (DI) water (the limit of detection (LOD) was 100 pM) and in the blood-like sample (the LOD was 1 nM).

2. Materials and methods

2.1. Materials

Gold (III) chloride trihydrate, hexadecyltrimethylammonium bromide (CTAB), sodium borohydride, ascorbic acid, silver

nitrate, D-penicillamine, hydrogen peroxide (H_2SO_4), sulfuric acid (H_2O_2) and 3-aminopropyltrimethoxysilane solution were purchased from Sigma-Aldrich. Reagents were dispersed in DI water. Polyethylene glycol (CM-PEG-SH, MW: 5000) was purchased from Laysan Bio, Inc.

2.2. Synthesis of GNR

Uniform GNR were synthesized using a seed-mediated growth method, as indicated in a previously published protocol with some modifications [23]. In brief, to prepare the gold-seed solution, $250 \mu\text{L}$ of 10 mM gold (III) chloride trihydrate was added to 7.5 ml of 93 mM CTAB solution, and then 0.6 ml of 10 mM cold sodium borohydride was added to the mixture with vigorous stirring. The mixture was allowed to react for 2 min and then stored at room temperature for 3 h . The growth solution was prepared based on 9.5 ml of 93 mM CTAB solution, and then $80 \mu\text{L}$ of 10 mM silver nitrate solution, 0.5 ml of 10 mM gold (III) chloride trihydrate solution, $55 \mu\text{L}$ of 100 mM ascorbic acid solution, and $12 \mu\text{L}$ of the gold-seed solution were sequentially dropped into the CTAB solution. The mixture was stored at room temperature for 6 h . The resultant solution was centrifuged at $15\,000 \text{ rpm}$ for 30 min to remove excess CTAB molecules and re-dispersed in 5 ml of DI water. Polyethylene glycol (PEG)-coated GNR (PGNR) were prepared as outlined in our previous report [27]. To prepare the PGNR, the GNR were coated with hetero-bi-functionalized PEG as a stabilizer. Then, 50 mg of CM-PEG-SH was added to 5 ml of GNR solution (4.73 mM of Au) and the mixture was allowed to react for 48 h at room temperature. The resultant solution was centrifuged at $15\,000 \text{ rpm}$ for 30 min to remove unbound CM-PEG-SH molecules and re-suspended in 5 ml of DI water.

2.3. Fabrication of GNR-based nanoplasmonics

The nanoplasmonic substrates were fabricated using the nanoparticle adsorption method previously described in a published report [23]. Glass cover slides ($12 \text{ mm } \varnothing$) were cleaned in piranha solution (3: 1 = H_2SO_4 : 30% H_2O_2). After cleaning in piranha, the slides were thoroughly rinsed with DI water and dried. To coat the glass cover slides with the amino-group, the glass cover slides were then immersed in 5 ml of ethanol containing $100 \mu\text{L}$ of 3-aminopropyltrimethoxysilane solution for 24 h . After the reaction, the glass cover slides were successively rinsed with an excess of DI water and ethanol and then dried. Subsequently, the amino-group-coated glass cover slides were immersed in PGNR solution (0.473 mM of Au) for 24 h , rinsed with DI water, and dried. Here, DPA-conjugated nanoplasmonic substrates were prepared using pre-fabricated PGNR-coated nanoplasmonic substrates with the addition of 1 ml of $1 \mu\text{M}$ DPA for 24 h . After the reaction, the DPA-covered nanoplasmonics were rinsed with DI water and dried.

2.4. Setup of LSPR

The nanoplasmonic substrates were put into a homemade LSPR sensing system [23]. The LSPR sensing system was composed of a fiber-coupled quartz-tungsten-halogen lamp

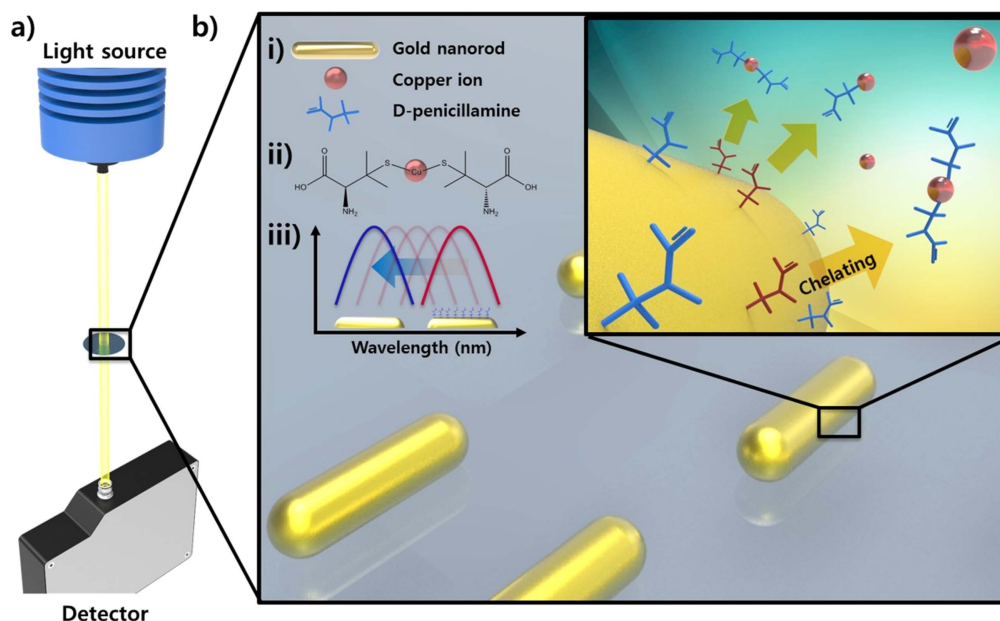


Figure 1. Schematic illustration of the recognition of copper II ions by localized surface plasmon resonance (LSPR). (a) Measuring process for the extinction spectrum of D-penicillamine- (DPA) conjugated gold nanorod (GNR) substrate. (b) Schematic illustration of the chelation of DPA and copper II ions on a GNR-based nanoplasmonic substrate. (i) Symbols for GNR, copper II ions, and DPA. (ii) Molecular formation of the chelation of DPA and copper II ions. (iii) Blue-shift in the extinction spectrum of the substrate after the chelation of DPA and copper II ions.

with a collimating lens and tilting mirror to change the beam path of the light source to the vertical direction, which can irradiate the bottom of the surface of a nanoplasmonic substrate. Finally, the irradiated light was collimated by the focusing lens to a portable spectrometer (figure 1(a)).

2.5. Selectivity test for copper II ions in a blood-like environment

For the selectivity test of copper II ions using nanoplasmonics, various metal ions, such as Fe^{2+} , Mn^{2+} , Na^+ , Ca^{2+} , Zn^{2+} and Ag^+ , were prepared at the same copper II ion concentration (1 nM). Furthermore, to investigate the potential of the DPA-covered nanoplasmonics for a blood-like environment, HSA was added to the sample solution. The final concentration of each metal ion and HSA was adjusted to 1 nM and 40 g L^{-1} in the sample solution.

3. Results and discussion

First, we fabricated GNR-based nanoplasmonics for the recognition of copper II ions. The nanoplasmonics was positioned between the light source and the detector (figure 1(a)). In our method, DPA plays a key role because it acts as a chelating agent for the copper II ions (figure 1(b)). It is known that two DPA molecules can chelate copper II ions, as shown in figure 1(b), and that the reaction leads to the detachment of the DPA from the surface of the GNR. This results in a blue-shift of the extinction signals, and the degree of the blue-shift quantifies the copper II ions. Furthermore, we selected GNR as the sensing elements on the nanoplasmonics

because GNR possess unique optical characteristics, such as a highly sensitive refractive index (RI) and tunable wavelength band which can be achieved by adjusting their aspect ratio. Thereby GNR exhibit excellent properties for an LSPR nanosensor without DPA [28].

The GNR were synthesized by previously published protocols with some modifications [23]. To immobilize the GNR to the glass substrate effectively, we prepared PGNR (figure 2(a)). The end-terminals of the PEG were made of thiol and carboxyl groups. The thiol functionalized PEG was conjugated with the surface of the GNR, therefore, the surface of the GNR was modified to a carboxyl group-terminated PEG. After preparation of the PGNR, we observed the size and morphology of the GNR and the PGNR using a transmission electron microscope (Jeol 1010) (figure 2(b)). We determined that the transverse length of the PGNR was $10.5 \pm 0.8 \text{ nm}$ and the longitudinal length was $36.1 \pm 1.2 \text{ nm}$ ($n = 100$). From these results, the aspect ratio of the PGNR was calculated to be approximately 3.5. The absorbance spectra of the GNR and the PGNR, which were dispersed in DI water, were measured by an ultraviolet–visible spectrometer (figure 2(c)) (UV-1800, Shimadzu). For the GNR, CTAB molecules surrounded the GNR, and a number of CTAB molecules existed in the DI water. Therefore, GNR can be dispersed in DI water through electrostatic repulsion. The absorbance peaks of the GNR were at 805 nm and 510 nm. However, some residue spectrum appears above a wavelength of 900 nm due to the CTAB. For the PGNR, absorbance peaks of the PGNR were at 789 nm and 510 nm. It is well-known that a red-shift is caused by an attachment of specific molecules on the surface of a metal nanoparticle; however, in our case, a blue-shift was observed which was

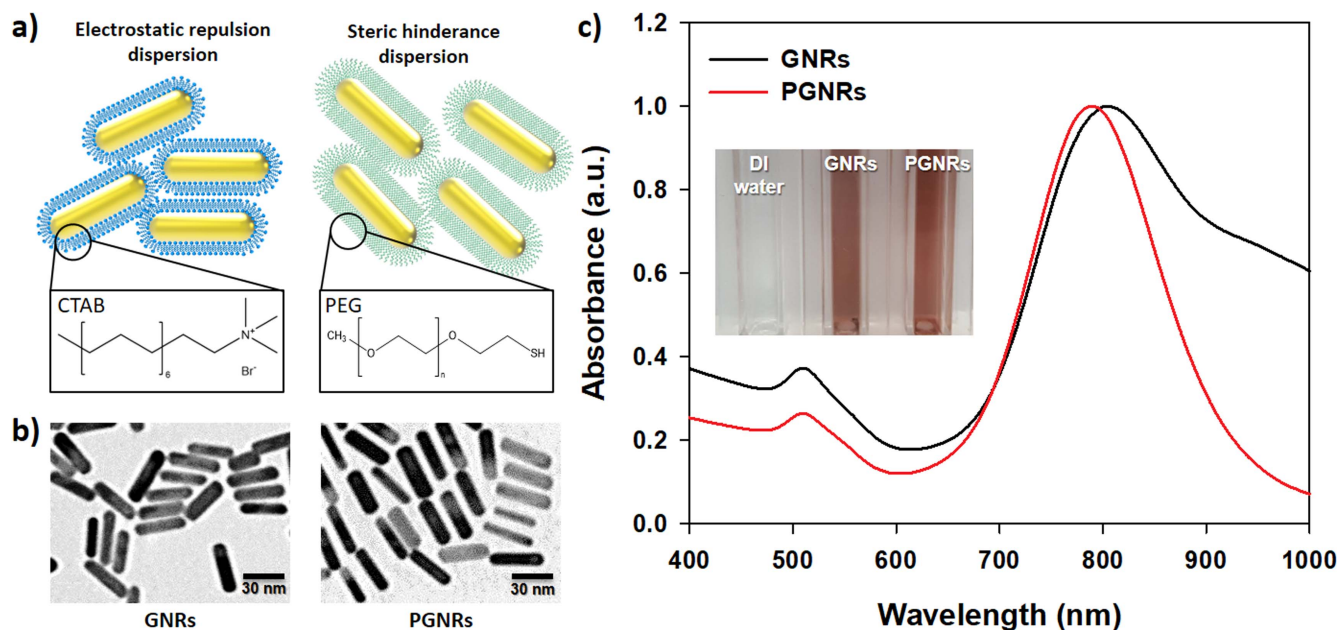


Figure 2. (a) Schematic illustrations of CTAB-coated GNR (left) and PEG-coated GNR (right). (b) Transmission electron microscopic images of GNR. The left image is bare GNR and the right image is PEG-coated GNR (PGNR). (c) Absorbance spectra of GNR and PGNR. Inset: a photograph of the GNR and PGNR.

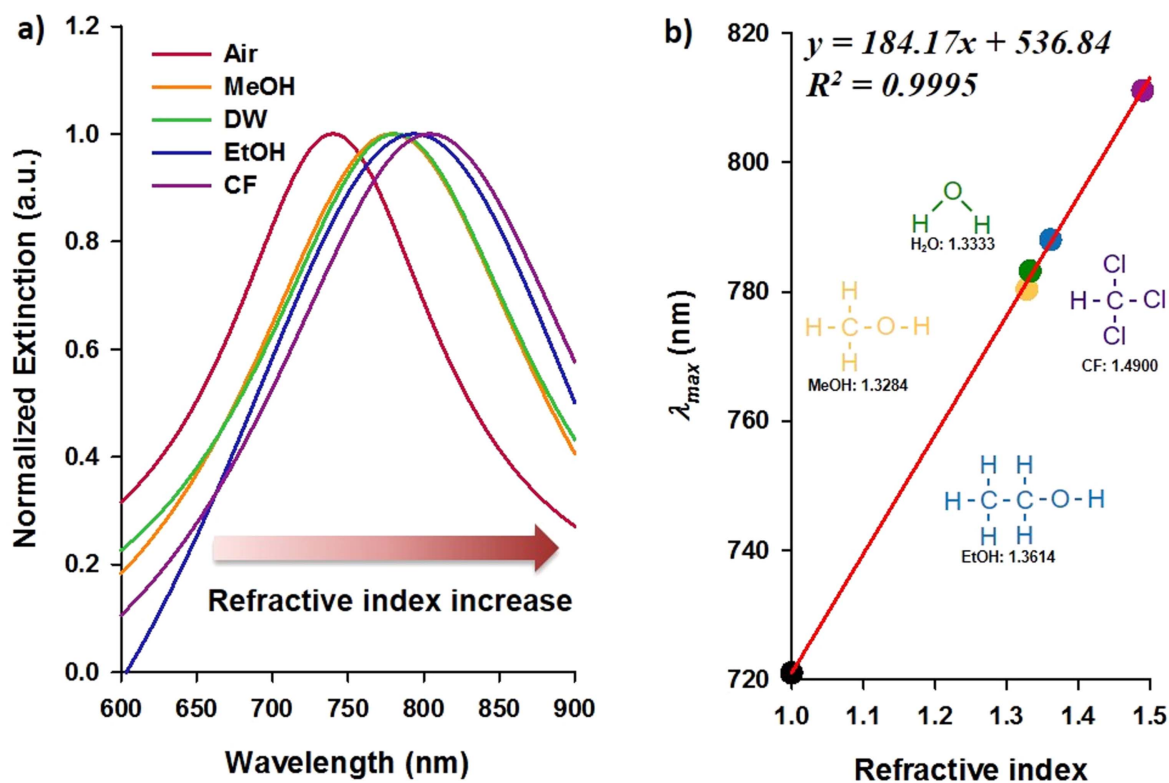


Figure 3. (a) Extinction spectra of attached PGNR on a glass substrate in different solvents. (b) The maximum wavelength of extinction spectra in (a) according to different refractive indexes of solvents.

possibly due the removal of an excess of CTAB molecules for longitudinal peaks in the absorbance spectra between GNR and PGNR. Furthermore, the relationship between the aspect ratio and the positions of the peaks of the PGNR showed good agreement. The absorbance peaks were generated at visible and near-infrared regions because of the collective

oscillation of electrons surrounding the GNR and the PGNR along the longitudinal and the transverse axes of the GNR and the PGNR respectively. After the preparation of the GNR and PGNR, colloidal stabilities were also investigated (inset of figure 2(c)). As shown in the inset of figure 2(c), the colors of the GNR and PGNR were almost the same (reddish-brown),

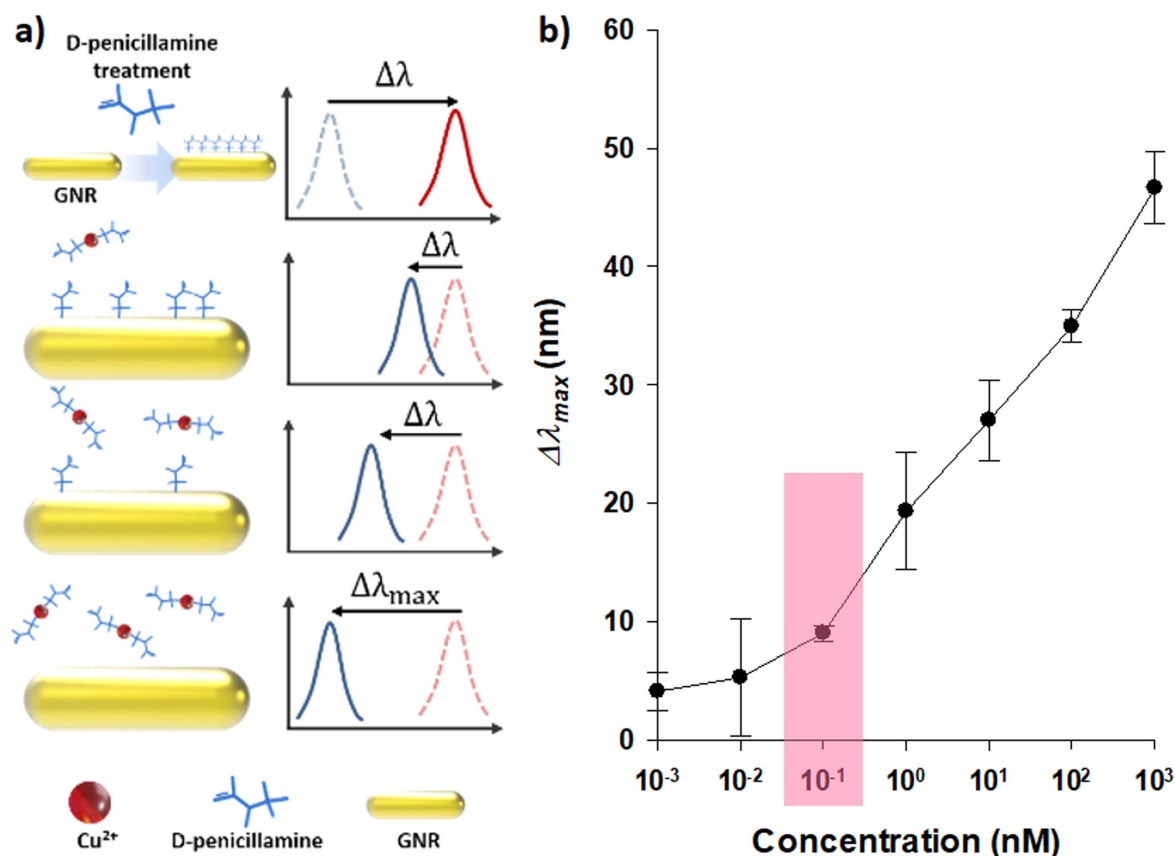


Figure 4. (a) Schematic illustration of the sensing mechanism using GNR-based nanoplasmonics for copper II ion detection. (b) Shift in maximum wavelength ($\Delta\lambda_{max}$) in the extinction spectra of nanoplasmonic substrates depending on changes in the concentration of copper II ions. The shaded red box represents the limit of detection (LOD) for GNR-based nanoplasmonics.

indicating excellent solubility for the DI water and colloidal stabilities without any aggregation and precipitation for over 30 days. Collectively, these results suggest that the PGNR as sensing elements for a nanoplasmonic substrate were uniformly synthesized, and the prepared PGNR demonstrated the potential for sensitive and precise LSPR sensing for the recognition of copper II ions.

Before the copper II ion detection using GNR-based nanoplasmonics, we investigated the sensitivity of a bare PGNR-coated nanoplasmonic substrate (before the DPA conjugation) (figure 3(a)). As shown in previously published reports [29–31], the sensitivity of LSPR-based sensing substrates was investigated depending on the change in the RI using various dielectric media with a different RI (air: 1.000, methanol: 1.328, water: 1.333, ethanol: 1.361, and chloroform: 1.490). When the RI of the dielectric media was increased, the position of the peak wavelength of extinction was red-shifted. Subsequently, the sensitivity toward the change in the RI of the surrounding dielectric media was also calculated for the bare PGNR-coated nanoplasmonic substrate, and the sensitivity of the nanoplasmonic substrate yielded 184.17 nm/RI unit (figure 3(b)). This sensitivity is comparable to previously published reports using the extinction of the ensemble of the GNR. From these results, we confirmed that prepared bare PGNR-coated nanoplasmonics can be applied to detect a low concentration of

biomolecules, such as copper II ions, by varying the surrounding RI of bare PGNR.

Subsequently, the copper II ion detection capability of the nanoplasmonics was investigated (figure 4(a)). As mentioned earlier, DPA plays a key role in the sensing mechanism of our sensing system. As shown in figure 4(a), DPA was detached from the PGNR due to the chelation with copper II ions. The detachment of the DPA from the surface of the GNR caused a blue shift. The detachment of the DPA from the surface of the GNR caused a blue shift. First, the extinction spectra were measured from the nanoplasmonic substrate after DPA conjugation in DI water with various concentrations (figure S1 is available online at stacks.iop.org/NANO/29/215501/mmedia). The extinction spectrum of the DPA-conjugated nanoplasmonic substrate was red-shifted to a maximum of 21.2 nm by 100 nM of DPA from the bare PGNR-coated nanoplasmonic substrate. In order to carry out a quantitative analysis of copper II ion detection, the extinction spectra were analyzed with various concentrations of copper II ions using DPA-conjugated nanoplasmonics (figures 4(b), S2). Based on the maximum wavelength (λ_{max}) blue-shift of the extinction spectra due to the detachment of the DPA from the surface of the PGNR, we confirmed that the efficiency of the detection of copper II ions was dominantly determined by the concentration of copper II ions. As the concentration of copper II ions increased, λ_{max} blue-shift of

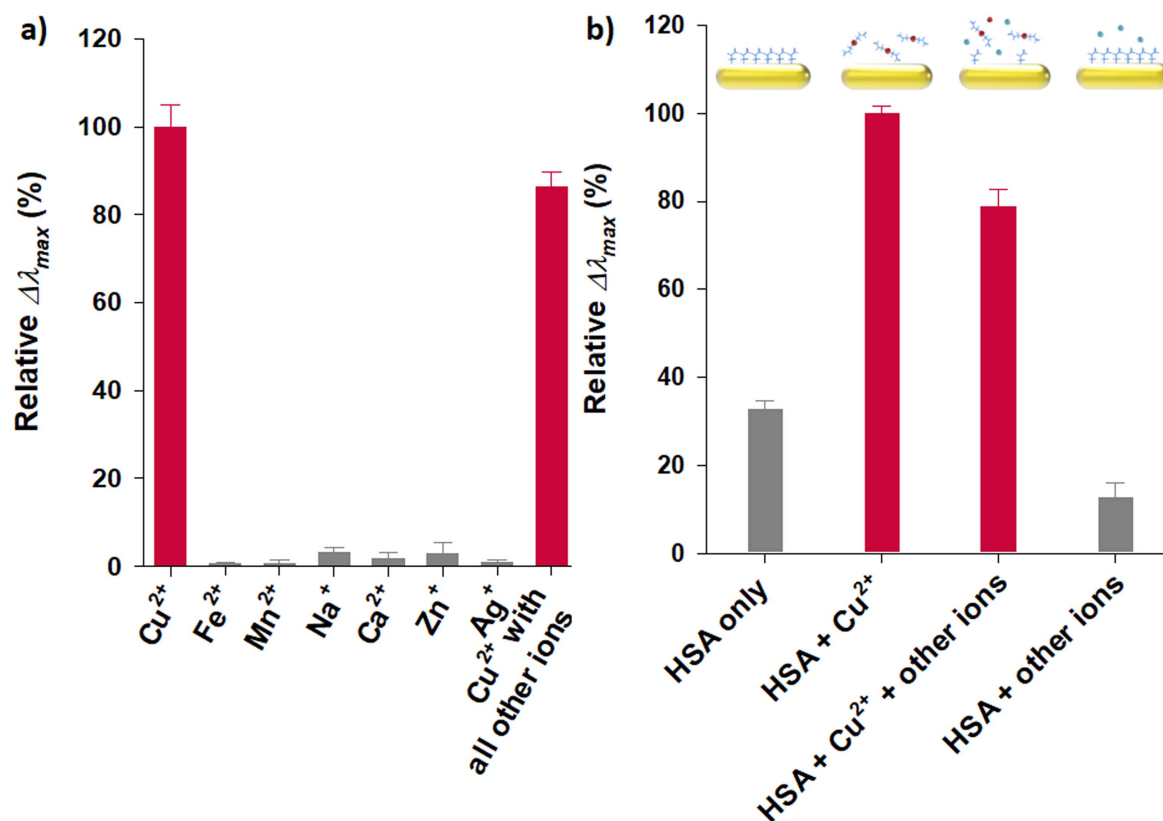


Figure 5. (a) Relative shift of the maximum wavelength ($\Delta\lambda_{\max}$) in the extinction spectra of nanoplasmonic substrates for indicated ions, including copper II ions. (b) $\Delta\lambda_{\max}$ in the extinction spectra of nanoplasmonic substrates for a human blood-like environment. The sample solution was mixed with human serum albumin (HSA, 40 g L^{-1}) and 1 nM of various ions. ‘HSA only’ represents the sample solution containing only HSA. ‘HSA + Cu^{2+} ’ represents the sample solution containing HSA and copper II ion. ‘HSA + Cu^{2+} + other ions’ represents the sample solution containing HSA and ions (Cu^{2+} , Fe^{2+} , Mn^{2+} , Na^+ , Ca^{2+} , Zn^{2+} and Ag^+). ‘HSA + other ions’ represents the sample solution containing HSA and ions (Fe^{2+} , Mn^{2+} , Na^+ , Ca^{2+} , Zn^{2+} and Ag^+) without copper II ions.

extinction spectra also increased. Moreover, the dynamic range of the nanoplasmonic substrate was from $1 \mu\text{M}$ – 100 pM . There was a large standard deviation of the blue-shift of the peaks in the extinction spectrum at 0.01 nM ($4.0 \pm 6.4 \text{ nm}$); therefore, the LOD was determined to be 100 pM ($9.1 \pm 0.6 \text{ nm}$). This LOD value for the nanoplasmonic substrate was higher than the inductively coupled plasma mass spectrometer [14] and the atomic absorption spectrometer [16] analytical method by approximately a factor of 10 to 1000.

Furthermore, a selectivity test for copper II ions was also carried out for DPA-covered nanoplasmonics with various ions (figures 5(a) and S3). Besides the copper II ions, biologically and environmentally affected metal ions were selected, such as Fe^{2+} , Mn^{2+} , Na^+ , Ca^{2+} , Zn^{2+} and Ag^+ , at an identical concentration of 1 nM. The percentage of the relative blue-shift of the peak was determined to be % relative $\Delta\lambda_{\max} = \Delta\lambda_{\max}$ for other ions / $\Delta\lambda_{\max}$ for 10 nM of copper II ions. For the other ions, changes in the blue-shift of the peak were scarcely observed compared to copper II ions, which have better selectivity compared with our previous research. [32, 33]. From these results, the developed sensing strategy is considered suitable for the detection of copper II ions using a DPA-conjugated nanoplasmonic substrate down to 100 pM , and the selectivity to copper II ions was also verified.

Finally, sensitivity tests for the nanoplasmonic substrate in a blood-like environment were conducted using HSA (figures 5(b) and S4). The concentration of HSA was set to 40 g L^{-1} because the reference range for the concentration of HSA is typically between 35 – 50 g L^{-1} [34]. The sample solution was prepared by mixing with copper II ions or other ions. For the sample solution containing only HSA, a negligible value for the blue-shift of the peak was exhibited ($10.96 \pm 0.56 \text{ nm}$) because of disulfide bonding between the DPA and albumin [35]. On the other hand, the sample solution containing HSA as well as 1 nM of copper II ions exhibited a significant blue-shift of the peak ($33.4 \pm 0.53 \text{ nm}$). Furthermore, the sample solution containing HSA with a mixture of 1 nM of Fe^{2+} , Mn^{2+} , Na^+ , Ca^{2+} , Zn^{2+} and Ag^+ , consecutively, showed a smaller blue-shift than the HSA only state because of the structural change of albumin ($4.26 \pm 1.11 \text{ nm}$). The structural change of albumin occurs with metal ions which decrease the binding affinity of HSA and DPA [36]. A sample solution containing HSA and copper II ions with other ions (Fe^{2+} , Mn^{2+} , Na^+ , Ca^{2+} , Zn^{2+} and Ag^+) was also prepared, and the resultant blue-shift of the peak was $27.5 \pm 1.28 \text{ nm}$. These results provide the potential to distinguish a biologically meaningful concentration (tens of μM) of copper II ions in human blood conditions through a blue-shift of the peak in the extinction spectrum using

DPA-conjugated nanoplasmonic substrates. From these data, our plasmonic sensor demonstrates the potential to detect heavy metal ions, such as mercury, cadmium, and lead [34, 37, 38].

4. Conclusions

We developed GNR-based nanoplasmonics covered with DPA as a chelating agent for the sensitive and selective sensing of copper II ions. As the DPA chelated to the copper II ions, the DPA was detached from the surface of the GNR. This behavior resulted in a blue-shift in the extinction spectrum of the GNR-based nanoplasmonics. Using this mechanism, copper II ions were recognized down to 10 pM in DI water and 1 nM in serum protein containing media. Thus, the GNR-based nanoplasmonics covered with DPA shows great potential as a sensing tool-kit for the recognition of specific ions using the LSPR effect, even under blood-like environments.

Acknowledgments

This work was supported by the National Research Foundation of Korea (NRF) grant, funded by the Korean government (NRF-2015R1A1A1A05027581, NRF-2017R1E1A1A01075439 and NRF-2017M3A9F1031229), 6-2014-0032, HI16C0179.

ORCID iDs

Jinsung Park  <https://orcid.org/0000-0001-8096-7286>
Jaemoon Yang  <https://orcid.org/0000-0001-7365-0395>

References

- [1] Stohs S J and Bagchi D 1995 Oxidative mechanisms in the toxicity of metal ions *Free Radical Biol. Med.* **18** 321–36
- [2] Valko M, Morris H and Cronin M T D 2005 Metals, toxicity and oxidative stress *Curr. Med. Chem.* **12** 1161–208
- [3] Schützendübel A and Polle A 2002 Plant responses to abiotic stresses: heavy metal-induced oxidative stress and protection by mycorrhization *J. Exp. Bot.* **53** 1351–65
- [4] Kochian L V 1995 Cellular mechanisms of aluminum toxicity and resistance in plants *Ann. Rev. Plant Physiol. Plant Mol. Biol.* **46** 237–60
- [5] Park J, Lee S, Jang K and Na S 2014 Ultra-sensitive direct detection of silver ions via Kelvin probe force microscopy *Biosens. Bioelectron.* **60** 299–304
- [6] Kodama H and Fujisawa C 2009 Copper metabolism and inherited copper transport disorders: molecular mechanisms, screening, and treatment *Metallomics* **1** 42–52
- [7] Zowczak M, Iskra M, Torliński L and Cofta S 2001 Analysis of serum copper and zinc concentrations in cancer patients *Biol. Trace Elem. Res.* **82** 1
- [8] Vural H, Demirin H, Kara Y, Eren I and Delibas N 2010 Alterations of plasma magnesium, copper, zinc, iron and selenium concentrations and some related erythrocyte antioxidant enzyme activities in patients with Alzheimer's disease *J. Trace Elem. Med. Biol.* **24** 169–73
- [9] Zumkley H B H P and Lison A 1979 Aluminium, zinc and copper concentrations in plasma in chronic renal insufficiency *Clin. Nephrology* **12** 18–21
- [10] Ala A, Walker A P, Ashkan K, Dooley J S and Schilsky M L 2007 Wilson's disease *Lancet* **369** 397–408
- [11] Bull P C, Thomas G R, Rommens J M, Forbes J R and Cox D W 1993 The Wilson disease gene is a putative copper transporting P-type ATPase similar to the Menkes gene *Nat. Genet.* **5** 327
- [12] Brady D C et al 2014 Copper is required for oncogenic BRAF signalling and tumorigenesis *Nature* **509** 492
- [13] Garber K 2015 Targeting copper to treat breast cancer *Science* **349** 128–9
- [14] Milne A, Landing W, Bizimis M and Morton P 2010 Determination of Mn, Fe, Co, Ni, Cu, Zn, Cd and Pb in seawater using high resolution magnetic sector inductively coupled mass spectrometry (HR-ICP-MS) *Anal. Chim. Acta* **665** 200–7
- [15] Pu X, Jiang Z, Hu B and Wang H 2004 [gamma]-MPTMS modified nanometer-sized alumina micro-column separation and preconcentration of trace amounts of Hg, Cu, Au and Pd in biological, environmental and geological samples and their determination by inductively coupled plasma mass spectrometry *J. Anal. At. Spectrom.* **19** 984–9
- [16] Fang Z, Guo T and Welz B 1991 Determination of cadmium, lead and copper in water samples by flame atomic-absorption spectrometry with preconcentration by flow-injection on-line sorbent extraction *Talanta* **38** 613–9
- [17] Zhang Z, Li W, Zhao Q, Cheng M, Xu L and Fang X 2014 Highly sensitive visual detection of copper (II) using water-soluble azide-functionalized gold nanoparticles and silver enhancement *Biosens. Bioelectron.* **59** 40–4
- [18] Vopálenská I, Váchová L and Palková Z 2015 New biosensor for detection of copper ions in water based on immobilized genetically modified yeast cells *Biosens. Bioelectron.* **72** 160–7
- [19] Deng H-H, Zhang L-N, He S-B, Liu A-L, Li G-W, Lin X-H, Xia X-H and Chen W 2015 Methionine-directed fabrication of gold nanoclusters with yellow fluorescent emission for Cu²⁺ sensing *Biosens. Bioelectron.* **65** 397–403
- [20] Xu M, Gao Z, Wei Q, Chen G and Tang D 2015 Hemin/G-quadruplex-based DNAzyme concatamers for *in situ* amplified impedimetric sensing of copper(II) ion coupling with DNAzyme-catalyzed precipitation strategy *Biosens. Bioelectron.* **4** 1–7
- [21] Mayer K M and Hafner J H 2011 Localized surface plasmon resonance sensors *Chem. Rev.* **111** 3828–57
- [22] Qing Z, Zhu L, Yang S, Cao Z, He X, Wang K and Yang R 2016 *In situ* formation of fluorescent copper nanoparticles for ultrafast zero-background Cu²⁺ detection and its toxicides screening *Biosens. Bioelectron.* **78** 471–6
- [23] Hong Y, Ku M, Lee E, Suh J-S, Huh Y-M, Yoon D-S and Yang J 2013 Localized surface plasmon resonance based nanobiosensor for biomarker detection of invasive cancer cells *J. Biomed. Optics* **19** 051202
- [24] Hormozi-Nezhad M R and Abbasi-Moayed S 2014 A sensitive and selective colorimetric method for detection of copper ions based on anti-aggregation of unmodified gold nanoparticles *Talanta* **129** 227–32
- [25] Yuan Z, Cai N, Du Y, He Y and Yeung E S 2014 Sensitive and selective detection of copper ions with highly stable polyethyleneimine-protected silver nanoclusters *Anal. Chem.* **86** 419–26
- [26] Brewer G J, Terry C A, Aisen A M and Hill G M 1987 Worsening of neurologic syndrome in patients with Wilson's disease with initial penicillamine therapy *Arch. Neurology* **44** 490–3
- [27] Eugene L, Yoochan H, Jihye C, Seungjoo H, Jin-Suck S, Yong-Min H and Jaemoon Y 2012 Highly selective

- CD44-specific gold nanorods for photothermal ablation of tumorigenic subpopulations generated in MCF7 mammospheres *Nanotechnology* **23** 465101
- [28] Cao J, Sun T and Grattan K T V 2014 Gold nanorod-based localized surface plasmon resonance biosensors: A review *Sensors Actuators B* **195** 332–51
- [29] Yoochan H, Eugene L, Minhee K, Jin-Suck S, Dae Sung Y and Jaemoon Y 2016 Femto-molar detection of cancer marker-protein based on immuno-nanoplasmonics at single-nanoparticle scale *Nanotechnology* **27** 185103
- [30] McFarland A D and Van Duyne R P 2003 Single silver nanoparticles as real-time optical sensors with zeptomole sensitivity *Nano Lett.* **3** 1057–62
- [31] Mayer K M, Lee S, Liao H, Rostro B C, Fuentes A, Scully P T, Nehl C L and Hafner J H 2008 A label-free immunoassay based upon localized surface plasmon resonance of gold nanorods *ACS Nano* **2** 687–92
- [32] Kuewhan J, Juneseok Y, Chanhoo P, Hyunjun P, Jaeyeong C, Chang-Hwan C, Jinsung P, Howon L and Sungsoo N 2016 Ultra-sensitive detection of zinc oxide nanowires using a quartz crystal microbalance and phosphoric acid DNA *Nanotechnology* **27** 365501
- [33] Park J, Choi W, Jang K and Na S 2013 High-sensitivity detection of silver ions using oligonucleotide-immobilized oscillator *Biosens. Bioelectron.* **41** 471–6
- [34] Margaron M P and Soni N 1998 Serum albumin: touchstone or totem? *Anaesthesia* **53** 789–803
- [35] Joyce D A and Day R O 1990 D-penicillamine and D-penicillamine-protein disulphide in plasma and synovial fluid of patients with rheumatoid arthritis *Br. J. Clin. Pharmacol.* **30** 511–7
- [36] Saha A and Yakovlev V V 2010 Structural changes of human serum albumin in response to a low concentration of heavy ions *J. Biophotonics* **3** 670–7
- [37] Kuchinskas E J and Rosen Y 1962 Metal chelates of dl-penicillamine *Arch. Biochem. Biophys.* **97** 370–2
- [38] Sugiura Y, Yokoyama A and Tanaka H 1970 Studies on the sulfur-containing chelating agents. XXIV. Acid dissociation and chelate formation of penicillamine *Chem. Pharm. Bull.* **18** 693–701